Figure 2.2.8
Curved mirror set to collimate the beam.

curvature of the mirror caused by its own weight. Even then, very careful mounting and precise mechanics are required to achieve this level of accuracy. If placed in the polychromatic beam directly from the source, cooling of the mirror will be necessary.

Other mirror arrangements can be employed, such as a horizontal and vertical pair of focusing mirrors in a Kirkpatrick–Baez (Kirkpatrick & Baez, 1948) arrangement. Such a device might be used to produce a small focal spot for powder-diffraction measurements from a sample in a diamond anvil cell. Multilayer mirrors can also be found in service on certain beamlines.

2.2.3.3. *Compound refractive lens*

The refractive index n of a material for X-rays is given (Gullikson, 2001; Spiller, 2000) by

$$n = 1 - \delta - i\beta = 1 - \frac{r_e}{2\pi}\lambda^2 \sum_n N_n f_n,$$

where $f_n = f_1 + if_2$ is the complex scattering factor for forward scattering for atom n and N_n is the number of atoms of type n per unit volume. δ and β are known as the refractive index decrement and the absorption index, respectively, and vary with photon energy depending on the proximity of an absorption edge. The real part of the refractive index is therefore slightly less than 1, with δ typically of the order 10^{-6}–10^{-9} depending on the energy. Thus a hole drilled in a piece of metal can act like a conventional convex lens, as the hole has a higher refractive index than the surrounding metal. With such a small difference in n between hole and metal, the focusing power is very slight; however, a series of holes (Fig. 2.2.9) can be used to focus the X-ray beam over a reasonable distance (Snigirev *et al.*, 1997, 1998). For a series of cylindrical lenses, the focal length, f, is given by $f = r/2N\delta$, where r is the radius of the hole and N is the number of holes.

Note that further away from the axis of the device the X-ray beam must pass through increasing amounts of material which absorb the radiation. Hence, only relatively small holes and apertures are possible (a maximum of a few mm in diameter) and weakly absorbing metals such as Be and Al are preferred. With hard-energy photons, Ni lenses are possible, and indeed the construction of such a device is a compromise between refractive power, absorption, aperture and the desired focal length. Such devices can be placed in the monochromatic beam or in a polychromatic beam with cooling.

Many variants of the basic scheme exist, with lenses pressed from foil with a parabolic form to eliminate spherical aberrations, with axial symmetry to focus in both the horizontal and vertical simultaneously (Lengeler *et al.*, 1999), etched *via* lithography from plastic or other material, or with a more complex profile to minimize the amount of redundant material attenuating the transmitted beam by absorption and so allowing a larger aperture. A 'transfocator' can be constructed whereby series of lenses can be accurately inserted or removed from the beam path, thus allowing the focusing power to be adjusted depending on the desired focal distance and the wavelength of the experiment (Vaughan *et al.*, 2011).

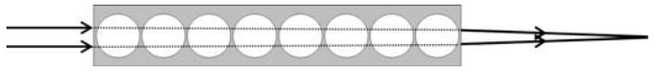

Figure 2.2.9
Schematic diagram of a set of refractive lenses.

2.2.4. Diffractometers

Most powder-diffraction beamlines are angle dispersive, operating with monochromatic radiation. When scanning a detector arm or employing a curved position-sensitive detector (PSD), detection is normally in the vertical plane because the polarization of the radiation in the plane of the synchrotron orbit means there is very little effect on the intensities due to polarization. By contrast, if diffracting in the horizontal plane, the projection of the electric vector onto the direction of the diffracted beam means that the intensity is reduced by a factor of $\cos^2 2\theta$, going to zero at $2\theta = 90°$, and so horizontal detection is less useful unless working at hard energies when 2θ angles are correspondingly small. In addition, for the highest angular resolution, the natural beam divergence in the vertical plane is usually lower than in the horizontal plane, particularly if the instrument has a bending magnet or wiggler as its source.

In general, diffractometers are heavy-duty pieces of equipment and are designed to have excellent angular accuracy while working with substantial loads. A high degree of mechanical accuracy is required to match the high optical accuracy inherent in the techniques employed. The calibration of the incident wavelength and any 2θ zero-point error is best done by measuring the diffraction pattern from a sample such as NIST standard Si (640 series), each of which has a certified lattice parameter (see Chapter 3.1). It is also good practice to measure the diffraction pattern of a standard sample regularly and whenever the instrument is realigned or the wavelength changed, to be sure that everything is working as expected.

Monochromatic instruments can have an analyser crystal or long parallel-foil collimators in the diffracted beam (a so-called parallel-beam arrangement), or can scan a receiving slit, or possess a one- or two-dimensional PSD, similar to Debye–Scherrer or Laue front-reflection geometry. Instruments equipped with a PSD can collect data much faster than those with a scanning diffractometer, so are exploited especially for time-resolved measurements. They may also have advantages for rapid data collection if the sample is sensitive to radiation, or be helpful if the sample is prone to granularity or texture to assess the extent of the problem.

Instruments can also be equipped with a sample changer, allowing measurements on a series of specimens, perhaps prepared by systematically changing the conditions of synthesis or the composition in a combinatorial approach. The use of beam time can be optimized with minimal downtime due to interventions around the instrument, and with the possibility to control the data acquisition remotely if desired.

2.2.4.1. *Parallel-beam instruments*

Cox *et al.* (1983, 1986), Hastings *et al.* (1984) and Thompson *et al.* (1987) described the basic ideas behind these instruments *via* their pioneering work at CHESS (Cornell, USA) and NSLS (Brookhaven, USA). The highly collimated monochromatic

incident beam is diffracted by the sample and passes *via* a perfect analyser crystal [such as Si or Ge(111)] to the detector. The analyser crystal defines a very narrow angular acceptance for the diffracted radiation, determined by its Darwin width. The combination of the collimation of the incident radiation, its highly monochromatic nature and the stringent angular acceptance defines the instrument's excellent angular resolution. The detector arm supporting the analyser is scanned through the desired range of 2θ angles either in a step-scan mode or continuously, reading out at very short intervals the electronic modules that accumulate the detector counts.

To be transmitted by the analyser crystal, a photon must be incident on the crystal at the correct angle θ_a that satisfies the Bragg condition. The analyser crystal defines therefore a true direction (2θ angle) for the diffracted beam irrespective of where in the sample it originates from. This removes a number of aberrations that affect diffractometers with a scanning slit or PSD where the 2θ angle is inferred from the position of the slit or detecting pixel. Thus, with a capillary specimen, peak widths are independent of the capillary diameter, so a fat capillary of non-absorbing sample can be used to optimize diffracted intensity, and any modest misalignment of the sample from the diffractometer axis, or specimen transparency or surface roughness for flat-plate samples, does not lead to shifts in the peak positions. Modest movement of the sample with temperature changes in a furnace *etc*. does not cause shifts in peak positions. These instruments are therefore highly accurate, and are ideal for obtaining peak positions for indexing a diffraction pattern of a material of unknown unit cell (the first step in the solution of a structure from powder data), or following the evolution of lattice parameter with temperature *etc*. For flat samples, the $\theta/2\theta$ parafocusing condition does not need to be satisfied to have high resolution. The peak width does not therefore depend on sample orientation, which is useful for measurements of residual strain by the $\sin^2\psi$ technique or for studying surfaces and surface layers by grazing-incidence diffraction. Interchange between capillary and flat-plate samples can easily be done as required without major realignment of the instrument. The stringent acceptance conditions also help to suppress parasitic scattering originating from sample-environment windows *etc*. and inelastic scattering such as fluorescence and Compton scattering.

On the other hand, at any 2θ angle only a tiny fraction of the diffracted photons can be transmitted by an analyser crystal, so this is a technique that consumes a lot of photons, and the high incident flux is essential to keep scan times to reasonable values. To overcome this, at least to some extent, Hodeau *et al.* (1998) devised a system of multiple analyser crystals, with nine channels mounted in parallel, each separated from the next by 2° (Fig. 2.2.10). In effect, as the detector arm is scanned, nine high-resolution powder-diffraction patterns are measured in parallel, each offset from the next by 2°. If the data from the channels are to be combined, which is the usual procedure, the detectors must be calibrated with respect to each other, in terms of counting efficiency and exact angular offset, by comparing regions of the diffraction pattern scanned by several detectors (Wright *et al.*, 2003). A multianalyser system speeds up data collection significantly and can be found in various modified forms at a number of powder-diffraction beamlines (*e.g.* Lee, Shu *et al.*, 2008).

The multianalyser approach is best suited to capillary samples because of the axial symmetry of the arrangement. With flat plates in reflection, only one detector can be in the $\theta/2\theta$ condition where the effect of specimen absorption (for a sufficiently thick sample) is isotropic. Corrections must therefore be made to the intensities from the other channels (Lipson, 1967; Koopmans & Rieck, 1968). For a capillary, choosing the wavelength and the diameter allows absorption to be kept to an acceptable value. Maximum diffracted intensity is expected at $\mu r = 1$ (where μ is the linear absorption coefficient and r the radius of the capillary), and below this value simple absorption corrections can be applied (Hewat, 1979; Sabine *et al.*, 1998). A value of μr greater than 1.5 begins to degrade the quality of the pattern significantly. If a sample with high absorption is unavoidable, such as when working close to an absorption edge of an element, *e.g.* the *K* edge of Mn at 6.539 keV (1.896 Å), then it can be preferable to stick a thin layer of sample on the outside of a 1-mm-diameter capillary. The shell-like nature of the sample has no effect on the peak shape or resolution because of the use of analyser crystals.

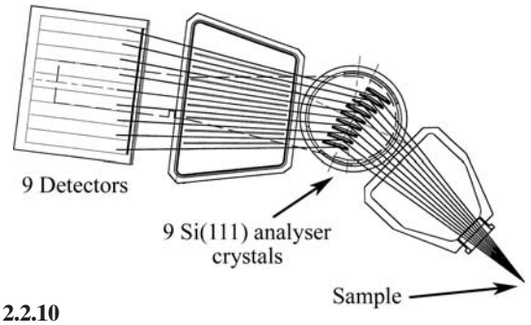

Figure 2.2.10
Multianalyser stage, nine channels separated by 2°, devised by Hodeau *et al.* (1998), originally installed on the BM16 bending-magnet beamline at the ESRF with Ge(111) analyser crystals. With an undulator source, the greatly increased flux allows use of Si(111), which has a narrower Darwin width (by a factor of ∼2.4) and thus improved 2θ resolution, but with a lower fraction of the diffracted radiation accepted.

Capillaries also have the advantage that preferred orientation can be significantly less as compared to a flat sample, where there is a tendency for crystallites to align in the surface layers, especially if compressed to hold the powder in place. Spinning or otherwise moving the sample is necessary, whether capillary or flat plate, to increase the number of crystallites appropriately oriented to fulfil the Bragg condition and avoid a spotty diffraction pattern, the likelihood of which is exacerbated by the highly collimated nature of the incident radiation.

2.2.4.1.1. *Angular resolution*

Various authors (*e.g.* Sabine, 1987*a*,*b*; Wroblewski, 1991; Masson *et al.*, 2003; Gozzo *et al.*, 2006) have discussed the resolution of a synchrotron-based diffractometer equipped with a double-crystal monochromator and an analyser crystal. The most usual setting of the diffracting crystals, ignoring any mirrors or other optical devices, is non-dispersive, alternatively described as parallel or (1, −1, 1, −1).

The approach developed by Sabine (1987*a*,*b*) involves modelling the vertical divergence of the source and the angular acceptance of the monochromator and analyser crystals as Gaussian distributions with the same full width at half-maximum (FWHM) as the real distributions, and considering a powder as a crystal with an infinite mosaic spread. The rocking curve of the analyser crystal (equivalent to rocking 2θ) is given by

$$I(\beta) = \int\int \mathrm{d}\alpha\,\mathrm{d}\delta \exp\left\{-\left[\left(\frac{\alpha}{\alpha'_m}\right)^2 + 2\left(\frac{\delta-\alpha}{\Delta'_m}\right)^2 + \left(\frac{b\delta+\alpha-\beta}{\Delta'_a}\right)^2\right]\right\},$$

where

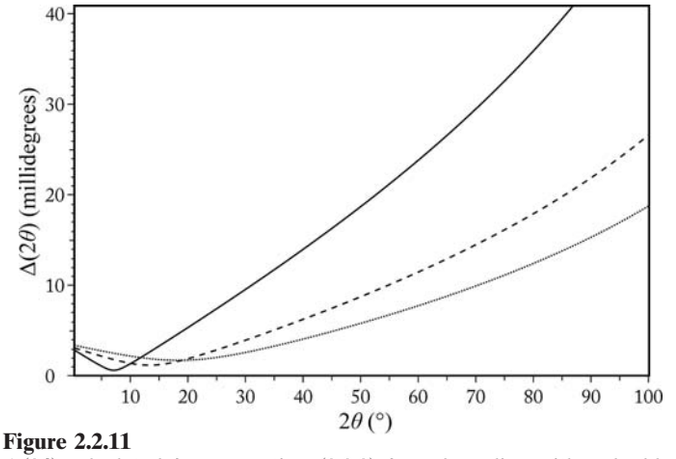

Figure 2.2.11
$\Delta(2\theta)$ calculated from equation (2.2.2) for a beamline with a double-crystal Si(111) monochromator, an Si(111) analyser ($\Delta_m = \Delta_a$ and $\theta_m = \theta_a$) and an FWHM vertical divergence of 25 μrad at $\lambda = 0.4$ Å (solid line: $\Delta_m \simeq 8.3$ μrad, $\theta_m = 3.6571°$), $\lambda = 0.8$ Å (dashed line: $\Delta_m \simeq 16.6$ μrad, $\theta_m = 7.3292°$) and $\lambda = 1.2$ Å (dotted line: $\Delta_m \simeq 25.2$ μrad, $\theta_m = 11.0319°$).

$$b = \tan\theta_a/\tan\theta_m - 2\tan\theta/\tan\theta_m.$$

Here α represents the vertical divergence from the source, δ is the difference between the Bragg angles of a central ray reflected from the monochromator at the angle θ_m and of another ray at angle θ'_m such that $\delta = \theta'_m - \theta_m$, and θ_a is the Bragg angle of the analyser crystal. The terms α'_m, Δ'_m and Δ'_a are related to the FWHM of the Gaussians representing the vertical divergence distribution or the Darwin widths of the monochromator and analyser crystals, α_m, Δ_m and Δ_a, respectively, with

$$\alpha'_m = \alpha_m/2(\ln 2)^{1/2}, \quad \Delta'_m = \Delta_m/2(\ln 2)^{1/2}, \quad \Delta'_a = \Delta_a/2(\ln 2)^{1/2}.$$

From the above equation, the intrinsic FWHM of the Gaussian-approximated peaks of the powder-diffraction pattern can be obtained as

$$\Delta^2(2\theta) = \alpha_m^2\left(\frac{\tan\theta_a}{\tan\theta_m} - 2\frac{\tan\theta}{\tan\theta_m} + 1\right)^2 + \tfrac{1}{2}\Delta_m^2\left(\frac{\tan\theta_a}{\tan\theta_m} - 2\frac{\tan\theta}{\tan\theta_m}\right) + \Delta_a^2. \quad (2.2.2)$$

Note that the true peak shape is not Gaussian, and a pseudo-Voigt (*e.g.* as described by Thompson *et al.*, 1987), Voigt (*e.g.* Langford, 1978; David & Matthewman, 1985; Balzar & Ledbetter, 1993) or other function modelled from first principles (*e.g.* Cheary & Coelho, 1992; Ida *et al.*, 2001, 2003) is usually better. Examples of FWHM curves calculated from equation (2.2.2) are plotted in Fig. 2.2.11 at three wavelengths. Differentiating the Bragg equation gives $\Delta d/d = -\cot\theta\,\Delta(\theta)$, where θ is in radians.

Gozzo *et al.* (2006) have extended the formulation of Sabine to include the effects of collimating and focusing mirrors in the overall scheme. Axial (horizontal) divergence of the beam between the sample and the detector causes shifts and broadening of the peaks, as well as the well known low-angle peak asymmetry due to the curvature of the Debye–Scherrer cones. Sabine (1987*b*), based on the work of Hewat (1975) and Hastings *et al.* (1984), suggests the magnitude of the broadening, $B(2\theta)$, due to horizontal divergence Φ can be estimated *via*

$$B(2\theta) = (\tfrac{1}{4}\Phi)^2(\cot 2\theta + \tan\theta_a),$$

where B and Φ are in radians. This value is added to $\Delta(2\theta)$.

2.2.4.1.2. *Hart–Parrish design*

A variant of the parallel-beam scheme replaces the analyser crystal with a set of long, fine Soller collimators (Parrish *et al.*, 1986; Parrish & Hart, 1987; Parrish, 1988; Cernik *et al.*, 1990; Collins *et al.*, 1992) (Fig. 2.2.12). The collimators define a true angle of diffraction, but with lower 2θ resolution than an analyser crystal because their acceptance angle is necessarily much larger and so the transmitted intensity is greater. They are not particularly suitable for fine capillary specimens, as the separation between foils may be similar to the capillary diameter, resulting in problems of shadowing of the diffracted beam. However, they are achromatic, and so do not need to be reoriented at each change of wavelength, which may have advantages when performing anomalous-scattering studies around an element's absorption edge. Unlike an analyser crystal, however, they do not suppress fluorescence. Peak shapes and resolution can be influenced by reflection of X-rays from the surface of the foils, or any imperfections in their manufacture, *e.g.* if the blades are not straight and flat. The theoretical resolution curve of such an instrument can be obtained from equation (2.2.2) by setting $\tan\theta_a$ to zero and replacing the angular acceptance of the analyser crystal Δ_a with the angular acceptance of the collimator Δ_c.

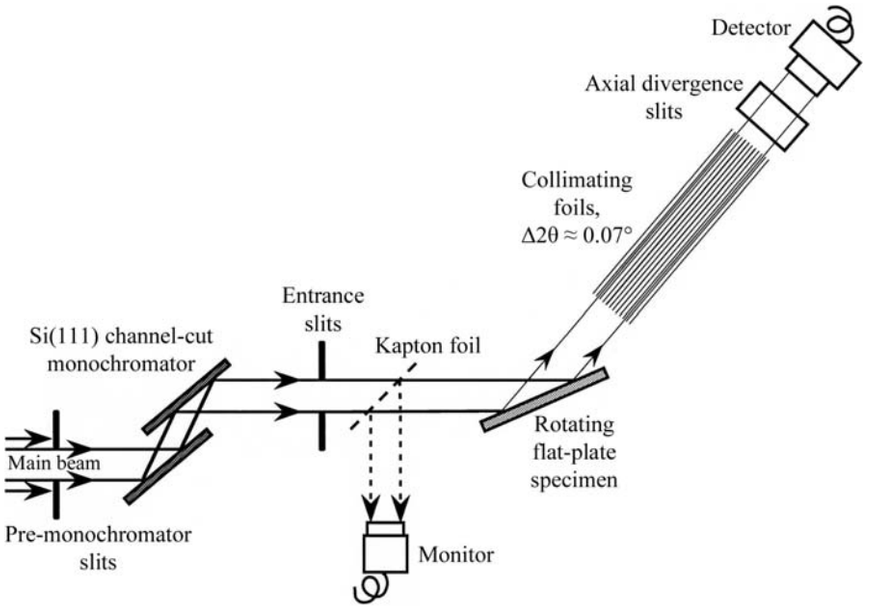

Figure 2.2.12
Schematic representation of a parallel-beam diffractometer of the Hart–Parrish design. The collimators installed on Stations 8.3 and 2.3 at the SRS Daresbury (Cernik *et al.*, 1990; Collins *et al.*, 1992) had steel blades 50 μm thick, 355 mm long, separated by 0.2 mm spacers, defining a theoretical opening angle (FWHM Δ_c) of 0.032° and a transmission of 80%.

2.2.4.2. *Debye–Scherrer instruments*

The simplest diffractometer has a receiving slit at a convenient distance from the sample in front of a point detector such as a scintillation counter. The height of the slit should match the capillary diameter, or incident beam height for flat plates. A slightly larger antiscatter slit near the sample should also be employed to reduce

references